AIChE

Near-Stoichiometric O_2 Binding on Metal Centers in Co(salen) Nanoparticles

Chad Johnson
Center for Environmentally Beneficial Catalysis, University of Kansas, Lawrence, KS 66047, and Dept. of Chemical and Petroleum Engineering, University of Kansas, Lawrence, KS 66045

Stefan Ottiger and Ronny Pini
ETH Zurich, Institute of Process Engineering, Sonneggstrasse 3, CH-8092 Zurich, Switzerland

Eric M. Gorman
Dept. of Pharmaceutical Chemistry, University of Kansas, Lawrence, KS 66047

Joseph G. Nguyen
Dept. of Chemistry, University of Kansas, Lawrence, KS 66045

Eric J. Munson
Dept. of Pharmaceutical Chemistry, University of Kansas, Lawrence, KS 66047

Marco Mazzotti
ETH Zurich, Institute of Process Engineering, Sonneggstrasse 3, CH-8092 Zurich, Switzerland

A. S. Borovik
Dept. of Chemistry, University of California, Irvine, CA 92697

Bala Subramaniam
Center for Environmentally Beneficial Catalysis, University of Kansas, Lawrence, KS 66047, and Dept. of Chemical and Petroleum Engineering, University of Kansas, Lawrence, KS 66045

DOI 10.1002/aic.11740
Published online February 26, 2009 in Wiley InterScience (www.interscience.wiley.com).

Co(salen) [cobaltous bis(salicylaldehyde)ethylenediamine] complexes are well-known O_2 carriers in solution. In the solid phase, these complexes exhibit some O_2 binding but detailed studies have been complicated because few of the known polymorphs of Co(salen) actually bind O_2. The O_2 binding results for nanoparticulate Co(salen) are presented in this study. Rod-shaped Co(salen) nanoparticles, roughly 100 nm in diameter, were recrystallized by spraying a methylene chloride solution of commercially obtained Co(salen) into supercritical carbon dioxide. Temperature-

Correspondence concerning this article should be addressed to B. Subramaniam at bsubramaniam@ku.edu.

programmed desorption, thermogravimetric analysis, and a Rubotherm magnetic suspension balance measurements reveal a reversible O_2 uptake of ~1.51 mmol/(g nanoparticles) at 25°C, consistent with a binding stoichiometry involving a bridging peroxo unit between two Co centers. In contrast, no measurable O_2 uptake was observed with the commercial Co(salen). These results clearly show the potential for bottom-up design of nanoparticulate metal complexes for enhanced O_2 storage and other applications. *AIChE J,* 55: 1040–1045, 2009
Keywords: O_2 binding, cobalt salen, nanoparticles

Introduction

Much of the work on O_2-binding transition metal complexes has been guided by attempts to mimic biological O_2-carriers, as outlined in several articles.[1–4] Cobaltous bis(salicylaldehyde)ethylenediamine (Co(salen)) and its derivatives are one class of complexes that have been extensively studied for their ability to reversibly bind O_2.[5–7] Co(salen) is the first reported synthetic reversible Co(II) oxygen carrier to bind O_2 in the solid state, and it is believed that the O_2 adduct consists of dimeric $[Co(salen)]_2O_2$ units.[8,9] However, there are several polymorphs of Co(salen), with only a few having the ability to bind O_2.[8,10] Formation of the different polymorphs is dependent on the preparative method, and heating and grinding can lead to interconversion between O_2 active and inactive forms.[8] Furthermore, a significant increase in O_2 affinity occurs when an additional ligand is coordinated to the Co(salen) complexes—for example, the formation of five-coordinate square pyramidal complexes promotes O_2 binding.[4,11]

Cobalt-O_2 carriers have been studied for a variety of applications in the solid state, focusing on O_2 separation and storage.[2,4] Compared to iron complexes, such as those with porphyrin ligands, cobalt complexes have shown more potential as O_2 sorbents for air separation.[2,4,12,13] Co(salen) complexes and its derivatives have been extensively studied for this application.[4] For example, the U.S. Air Force attempted to use the compound to sequester O_2 from air but technical obstacles, including slow oxygenation rates, irreversible oxidation, and sensitivity to moisture, have hampered successful utilization.[4]

We have used Co(salen) and its derivatives as homogeneous oxidation catalysts in solution,[14,15] and as oxygen carriers[11] and catalysts in porous polymeric hosts.[16,17] The complexes are sequestered in templated polymers to isolate the metal centers, thereby avoiding dimerization and improving the stability of the adsorbent.[11,13] More recently, nanoparticles of transition metal complexes, including Co(salen), were prepared using precipitation with compressed antisolvent (PCA) technology. In the PCA technique, nanoparticles of Co(salen) were precipitated from methylene chloride solution using supercritical CO_2 as an antisolvent. Scanning electron microscopy (SEM) showed that the processed Co(salen) nanoparticles have rod-like morphology with average diameters around 100 nm and lengths on the submicron scale.[18] Investigations into the O_2 binding properties of the Co(salen) particulates (Scheme 1) are presented in this report. Our findings show a greater O_2 binding capacity for the nanoparticles compared to their unprocessed analogs. Furthermore, our results support the formation of $[Co(salen)]_2O_2$ species within the nanoparticulates.

Materials and Methods

Co(salen) was purchased from Sigma-Aldrich and used as received. SEM characterization revealed that the particle size of this material was on the order of tens to hundreds of microns. Co(salen) nanoparticles were created as explained in previous work with a smaller precipitation vessel (0.95 L) as well as a SCEPTER® (Graver Separations) (0.1 μm) filter.[18] The oxygen used for the thermogravimetric analysis (TGA) studies was USP medical grade from Linweld while the N_2 utilized was boiled off from a liquid nitrogen dewar. The oxygen and helium utilized for the Rubotherm adsorption experiments were obtained from Pangas AG (Luzern, Switzerland) at purities of 99.95% and 99.999%, respectively. Argon for the temperature-programmed desorption (TPD) experiments was high purity grade (99.996%) from Linweld.

The true (skeletal) density analysis of both the commercial Co(salen) as well as Co(salen) nanoparticles was performed by Quantachrome Instruments using a gas-expansion pycnometer. Specific surface area and pore volume analyses of both materials were performed by NanoScale Materials.

TPD of the materials was carried out using Argon at 30 sccm. The powders [306 mg of the commercial Co(salen) and 8.3 mg of the Co(salen) nanoparticles] were loaded in a fixed bed arrangement into a quartz tube reactor and heated from room temperature to 200°C at 5°C/min for the Co(salen) nanoparticles and 6.7°C/min for the commercial Co(salen). The effluent gases were analyzed using a Pheiffer Vacuum mass spectrometer (Omnistar Quadrupole Mass Spectrometer Model GSD 300 02).

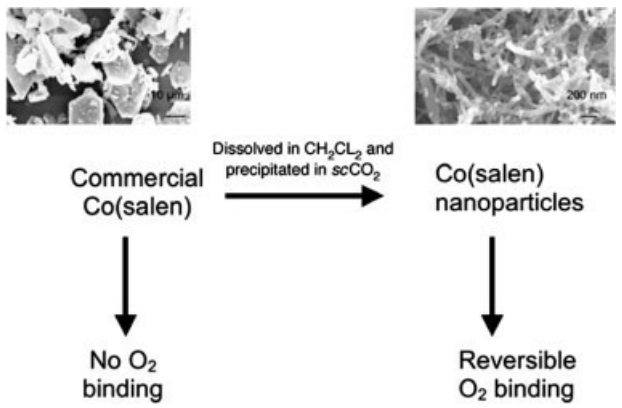

Scheme 1. Morphology and functional properties of Co(salen) recrystallized as nanoparticles.

The O_2 desorption data were collected with a TA Instruments Q50 Series Thermogravimetric Analyzer (TGA) with a heating rate of 5°C/min and balance with sample flow rates of 40 and 60 sccm, respectively. The TGA was also modified to perform O_2 binding studies utilizing the gas switching capability of the instrument. The sample [1.192–9.335 mg of the commercial Co(salen) and 0.717–2.245 mg of the Co(salen) nanoparticles] was first equilibrated at 60°C and held there for 5 min to desorb any O_2 that had bound during air exposure. Then, the furnace was cooled to 25°C and held for an additional 5 min. Following this step, the sample gas was changed automatically from the standard N_2 to O_2 (60 sccm). After a 30-min O_2 pulse, it was found that the mass change leveled off and the sample gas was switched back to N_2.

The static oxygen adsorption measurements were performed in a Rubotherm magnetic suspension balance (Rubotherm, Bochum, Germany), equipped with a calibrated sinker for an *in situ* measurement of the fluid density.[19] The Rubotherm balance allows one to measure the weight of the sample with an accuracy of 0.01 mg and can be operated at pressures and temperatures up to 450 bar and 250°C, respectively. The measuring cell is kept at a constant temperature with a heating jacket and temperature (T) is measured with a calibrated thermocouple at an accuracy of 0.1°C. Pressure (P) is measured using a pressure sensor PAA-35XHTT (Keller, Winterthur, Switzerland), which can measure up to 3 bar with an accuracy of 0.15% FS. More details of the experimental setup may be found elsewhere.[20,21] The sorbent samples [1728.38–1776.01 mg of the commercial Co(salen) and 166.83 mg of the Co(salen) nanoparticles] were kept in sealed glass beakers under an Argon atmosphere and were regenerated for at least 4 h under vacuum at 60 or 120°C before being used in the adsorption measurements.

After regeneration, the sorbent sample is placed in the basket, the magnetic suspension balance is evacuated and the weight $M_1^0 = m^{\text{met}} + m_0^{\text{sorb}}$ under vacuum is measured at a temperature of 25°C, where m^{met} and m_0^{sorb} represent the weights of the lifted metal parts and of the sorbent sample, respectively. Then, the system is filled with helium at a pressure of about 2 bar and the volume of the metal parts and the sorbent sample $V^{\text{met}} + V_0^{\text{sorb}}$ is obtained from the measured weight M_1 ($\rho_{\text{He}}^{\text{b}}$,$T$) and the density $\rho_{\text{He}}^{\text{b}}$:

$$V^{\text{met}} + V_0^{\text{sorb}} = \frac{M_1^0 - M_1(\rho_{\text{He}}^{\text{b}}, T)}{\rho_{\text{He}}^{\text{b}}}. \tag{1}$$

After evacuating it again, the cell is filled with oxygen and the weight M_1 (ρ^{b},T) is measured at the desired conditions, i.e., density ρ^{b} and temperature of 25°C:

$$M_1(\rho^{\text{b}}, T) = M_1^0 + m^{\text{a}} - \rho^{\text{b}}[V^{\text{met}} + V_0^{\text{sorb}} + V^{\text{a}}], \tag{2}$$

where m^{a} and V^{a} are the absolute amount adsorbed and the volume of the adsorbed phase, respectively. The latter cannot be directly measured, and the only measurable quantity is the excess adsorption $\Gamma(\rho^{\text{b}},T)$:

Table 1. Physical Properties of Unprocessed and Co(salen) Nanoparticles

	True Density (g/cc)	Surface Area (m^2/g)	Pore Volume (10^{-3} mL/g)
Commercial Co(salen)	1.6111	Too low to be measured	0.4
Co(salen)nanoparticles	1.3157	14–18	29–31

$$\Gamma(\rho^{\text{b}}, T) = m^{\text{a}} - \rho^{\text{b}} V^{\text{a}} = M_1(\rho^{\text{b}}, T) - M_1^0 + \rho^{\text{b}}[V^{\text{met}} + V_0^{\text{sorb}}]. \tag{3}$$

However, since the densities at which the measurements are performed are relatively low, the term $\rho^{\text{b}}V^{\text{a}}$ is much smaller than m^{a} and the absolute amount adsorbed can be approximated by the excess adsorption, $m^{\text{a}} \cong \Gamma$. Therefore, the experimental results are reported here in terms of the molar absolute adsorption n^{a} defined as follows:

$$n^{\text{a}}(\rho^{\text{b}}, T) = \frac{\Gamma(\rho^{\text{b}}, T)}{M_{\text{m}} m_0^{\text{sorb}}}, \tag{4}$$

where M_{m} represents the molar mass of the adsorbate.

Results and Discussion

Physical particle characterization

Electron paramagnetic resonance, electronic absorbance spectroscopies and elemental analysis (ICP) characterizations of the unprocessed Co(salen) and the processed nanoparticulates thereof produced similar spectral and analytical results, demonstrating that the metal complexes remain intact following precipitation.[18] However, as shown in Table 1, the true density of the nanoparticles is lower than that of the unprocessed Co(salen) by about 0.3 g/mL (18%). In addition, there are significant differences in the surface areas and pore volumes between the unprocessed and nanoparticulated forms of Co(salen) (Table 1). In particular, the Brunauer Emmett Teller (BET) measurements suggest that the nanoparticles of Co(salen) are porous, having an average pore volume of 30 $\times$ 10^{-3} mL/g of nanoparticles and mean pore diameter of 6–8 nm. The porosity is consistent with the lower true density of the nanoparticles.

Quantifying oxygen adsorption and desorption

The Co(salen) nanoparticles displayed a visible color change from brown to green upon exposure to air. In contrast, the unprocessed starting Co(salen) complex did not show any such color change when exposed to air. To verify that this color change was caused by enhanced O_2 binding, a TPD study was carried out on both samples after exposure to ambient O_2. As shown in Figure 1, the Co(salen) nanoparticles exhibited substantial O_2 desorption beginning around 35°C, whereas the unprocessed analog only displayed slight O_2 desorption at temperatures approaching 175°C. The observed TPD signal for the commercial Co(salen) is approximately an order of magnitude lower than the corresponding signal for the Co(salen) nanoparticles even though the amount of commercial Co(salen) used in the experiments is

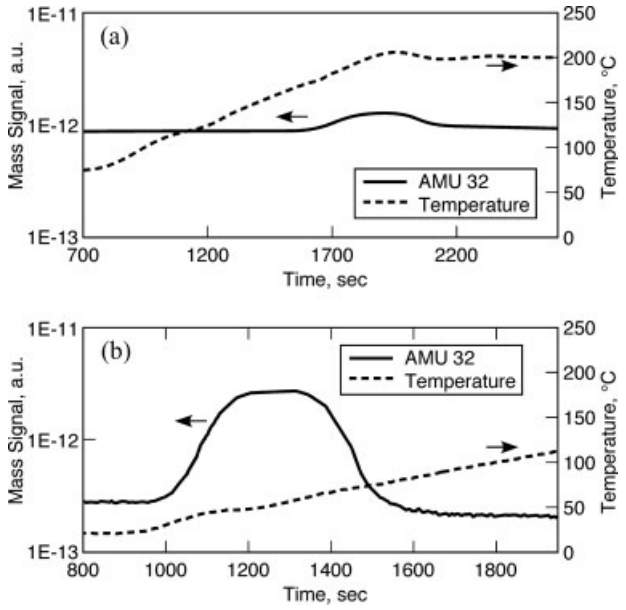

Figure 1. Temperature-programmed desorption profiles displaying mass signal, atomic mass unit (AMU) 32 (O_2) (—), and furnace temperature ramp (– – –): (a) commercial Co(salen); (b) air exposed Co(salen) nanoparticles.

an order of magnitude greater than the Co(salen) nanoparticles. Thus, when normalized with the amount of Co(salen) used in the TPD experiments, the mass of O_2 desorbed on the commercial Co(salen) is so low compared to that on the Co(salen) nanoparticles that additional experiments will be needed to reliably establish the intrinsic amount of O_2 desorbed from the commercial Co(salen). However, this was not our focus; rather, the purpose of the TPD experiments was to show that the bound O_2 in Co(salen) nanoparticles can indeed be desorbed with gentle heating.

TGA was utilized to further quantify the amount of O_2 bound to the samples. For the nanoparticle exposed to air, there was a 3–4% mass decrease with O_2 desorption starting at 32°C (Figure 2). As a control, the unprocessed Co(salen) was investigated and no mass change was observed as the sample was heated to 100°C.

To obtain additional quantitative information on the O_2 binding, including whether it is a reversible process, the TGA instrument was modified so that O_2 could be passed through the furnace in a continuous fashion. In a typical experiment, Co(salen) nanoparticles were exposed to air and then heated to 60°C to desorb the oxygen—this caused mass losses between 4 and 5% (Figure 3). The furnace was then cooled to room temperature and pure O_2 was continuously flowed through the furnace for ~30 min. As illustrated in Figure 3, the nanoparticles showed rapid O_2 uptake that ranged from 3 to 4% of the adsorbent mass, corresponding to an O_2 adsorption of 1.27 mmol of O_2/g of nanoparticle. Following the prolonged O_2 exposure, N_2 was purged through the furnace, causing the bonded O_2 to desorb. The control experiments with unprocessed Co(salen) showed no measurable gas adsorption.

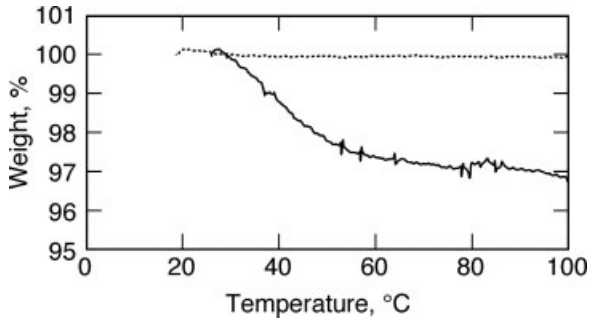

Figure 2. TGA desorption profiles corresponding to air exposed commercial Co(salen) (– – –) and Co(salen) nanoparticles (—).

To corroborate the TGA results, the unprocessed Co(salen) complex and the nanoparticulate Co(salen) were analyzed for O_2 adsorption at 25°C using a Rubotherm magnetic suspension balance. This experiment utilizes different pressures of O_2, with equilibrium being indicated by a negligible rate of mass change. Consistent with our other measurements, the unprocessed Co(salen) complex displayed no measurable binding of O_2. In contrast, significant O_2 binding was observed for the Co(salen) nanoparticles, whose experimental data are given in Table 2. Figure 4 shows the equilibrium O_2 adsorption isotherms on Co(salen) nanoparticles. Filled symbols refer to the experiments carried out in adsorption mode, whereas the empty symbols to the desorption runs. Before measurements, the sample has been regenerated under vacuum at 60°C (triangles) or at 120°C (circles), but no difference in the measured isotherms has been observed. As shown in Figure 4, the equilibrium O_2 adsorption isotherms display a sharp rise beyond 0.2 bar of O_2 pressure, attaining a saturation value of 1.51 mmol of O_2/g of nanoparticle at higher pressures—this change corresponds to a 5.1% mass increase based on the mass of the adsorbent. In addition, this quantity of O_2 uptake corresponds to 98% of the stoichiometric

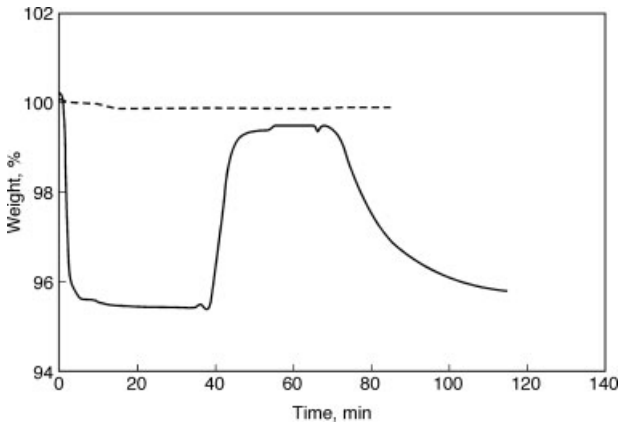

Figure 3. TGA profiles showing O_2 desorption into flowing N_2 (at 60°C) followed by subsequent (around 30 min) adsorption from flowing O_2 stream at room temperature (~20°C): commercial Co(salen) (– – –) and Co(salen) nanoparticles (—).

Table 2. Experimental Equilibrium O_2 Adsorption and Desorption Isotherms on Co(salen) Nanoparticles Measured at 25°C Using Two Different Regeneration Temperatures

T_{reg} (°C)	P (bar)	n^a (mmol/g)
60	0.103	0.002
	0.155	0.003
	0.164	0.934
	0.198	1.096
	0.411	1.45
	0.807	1.495
	0.2	1.488
	0.051	1.469
	0.031	1.322
	0.023	1.106
	0.004	0.049
120	0.06	0.001
	0.12	0.018
	0.15	0.728
	0.212	1.251
	0.317	1.39
	0.607	1.504
	1.019	1.512
	0.697	1.512
	0.449	1.516
	0.249	1.513
	0.1	1.504
	0.031	1.481

amount predicted for $[Co(salen)]_2O_2$ complexes. The formation of this dimeric structural motif within the Co(salen) nanoparticles is consistent with what is known for O_2 adducts in other solid forms of Co(salen).[8,9,22]

The desorption isotherm of the Co(salen) nanoparticles is also shown in Figure 4 and a lower O_2 pressure (0.005 bar) is required to completely desorb (less than sensitivity of instrument) the O_2 from the nanoparticles. The adsorption and desorption isotherms exhibit hysteresis, a property that has been observed previously for other Co(salen) systems. For instance, the five-coordinate Co(salen)(pyridine) complex also shows a hysteresis effect,[13] which has been attributed to a restructuring of the crystal lattice during desorption (Similar changes in phase were also observed in previous reports of Co(salen) and similar complexes).[12,23]

The O_2 binding properties of the Co(salen) nanoparticles are superior to other cobalt-based adsorbents (An early report describes a mass change of between 3.5 and 4.5% after exposure to O_2 at room temperature for solid Co(salen).[22] However, there were no experimental details associated with this report). For instance, the crystalline phase of the four-coordinate complex, $(Bu_4N)_2Co(CN)_4$, was reported to adsorb O_2—the quantity taken up corresponded to 91% of the stoichiometric amount that is predicted for a 1:1 Co-O_2 complex. However, this material lost only 56% of its adsorbed oxygen while purging with N_2 at 30°C.[12] The Co(salen) nanoparticles also outperformed five-coordinate Co(salen) complexes—these types of systems are known to have high affinities for O_2 in solution.[4] Nonetheless, only 1.06 mmol of O_2/g of solid was taken up by Co(salen)(pyridine) complex 25°C as measured by a static volumetric system.[13]

Recently, we have reported on the structure and ligand environment of the Co(salen) nanoparticles and commercial Co(salen), investigated by the combined application of infrared, Raman, X-ray absorption near edge structure (XANES), and extended X-ray absorption fine structure (EXAFS) spectroscopies in conjunction with X-ray diffraction (XRD) experiments before and during interaction with O_2.[24] The results indicate that the enhanced O_2 binding properties of Co(salen) nanoparticles are related to structural differences between the unprocessed Co(salen) and the Co(salen) nanoparticles. The spectroscopy results indicate the presence of Co^{II} centers with distorted tetrahedral geometry in the case of the Co(salen) nanoparticles and no evidence of metallic Co clusters, confirmed by the lack of Co—Co contributions at bonding distances in the EXAFS spectra and the presence of characteristic features of Co^{II} in the XANES spectra. The EXAFS data also indicate that there are on average two Co—N and two Co—O bonds with a distance of 1.81 ± 0.02 Å and 1.90 ± 0.02 Å, respectively, consistent with typical metal salen structures. Upon O_2 binding on the Co(salen) nanoparticles, the XANES results indicate oxidation of the Co^{II} to Co^{III}, consistent with the vibrational data showing new bands associated with oxygen species bonded to Co centers and the increase in the oxygen coordination number from 1.8 to 2.9 in the EXAFS data.

The dioxygen uptake by the nanoparticulate Co(salen) is ~1.51 mmol of oxygen per gram of nanoparticles, a value that is consistent with one O_2 molecule per two Co(salen) complexes. The structural characterization results are consistent with this bridging stoichiometry. The XANES results showed that upon exposure to O_2, the Co(salen) complexes within the nanoparticle are oxidized from Co^{II} to Co^{III}, a result that is consistent with dioxygen being reduced to a bridging peroxo moiety.[24] Further, the EXAFS results on O_2-treated nanoparticles indicated an increase in coordination number of the Co complexes from four to five compared to the original, untreated samples. The Raman vibrational band that appears for the O_2-exposed Co(salen) nanoparticles is in the region normally associated with bridging peroxo ligands

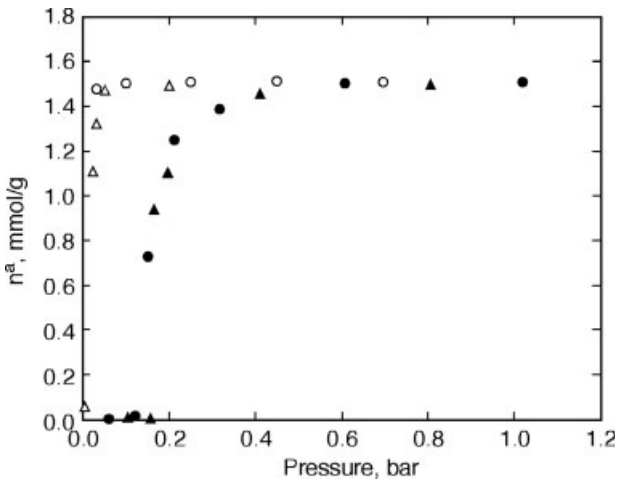

Figure 4. O_2 adsorption and desorption isotherms for Co(salen) nanoparticles at 25°C showing hysteresis (filled symbols refer to adsorption and empty symbols to desorption).

Before the measurement, the sample was regenerated at two different temperatures: 60°C (triangles) and 120°C (circles).

to cobalt complexes, providing further complementary evidence for the 2 Co:1 O_2 binding ratio.[24]

Conclusions

Co(salen) nanoparticles, precipitated from organic solution using dense carbon dioxide as the antisolvent, show enhanced and reversible O_2 binding relative to the unprocessed Co(salen), which shows no measurable O_2 binding. The adsorbed O_2 is desorbed by a stream of flowing inert gas, such as N_2 or Argon, at room temperature; in addition, heating above 30°C accelerates the desorption. The stoichiometry of binding suggests an O_2 to Co(salen) ratio of 1:2 that is consistent with the formation of a bridging peroxo unit between two Co centers. This structure is a well-known motif for metal complexes in solution.[25] However, it is somewhat surprising for a solid–gas reaction and could be related to an unusual arrangement of molecules within the Co(salen) nanoparticles. Nevertheless, the nearly quantitative O_2 uptake and its reversible desorption illustrates the potential of these nanoparticles as sorbents for gases.

Acknowledgments

The authors thank the NSF-ERC program (NSF-EEC 0310689) for financial support of this work as well as David Slade and Dr. Susan Williams for their help with the TPD studies.

Notation

m^a = absolute adsorption in mass units, g
m_0^{sorb} = initial weight of the sorbent sample, g
M_m = molar mass of adsorbate, g/mol
m^{met} = weight of the lifted metal parts, g
M_1 = weight at measuring point 1, g
M_1^0 = weight at measuring point 1 under vacuum, g
n^a = molar absolute adsorption per unit mass of sorbent, mmol/g
P = pressure, bar
T = temperature, K
V^{met} = volume of lifted metal parts, cm^3
V_0^{sorb} = volume of sorbent sample, cm^3
V^a = volume of the adsorbed fluid, cm^3

Greek letters

Γ = adsorption excess in mass units, g
ρ = density, g/cm^3

Subscripts and superscripts

b = bulk
He = helium

Literature Cited

1. Niederhoffer EC, Timmons JH, Martell AE. Thermodynamics of oxygen binding in natural and synthetic dioxygen complexes. *Chem Rev*. 1984;84:137–203.
2. Norman JA, Pez GP, Roberts DA. Reversible complexes for the recovery of dioxygen, In: Martell AE, Sawyer DT, editors. *Oxygen Complexes and Oxygen Activation by Transition Metals*. New York: Plenum Press, 1988:107–125.
3. Jones RD, Summerville DA, Basolo F. Synthetic oxygen carriers related to biological systems. *Chem Rev*. 1979;79:139–179.
4. Li GQ, Govind R. Separation of oxygen from air using coordination complexes: a review. *Ind Eng Chem Res*. 1994;33:755–783.
5. Pfeiffer P, Breith E, Lubbe E, Tsumaki T. Tricyclic ortho-condensed partial valence rings. *Justus Liebigs Ann Chem*. 1933;503:84–130.
6. Tsumaki T. Coordinate valency rings. IV. Some inner complex salts of hydroxyaldimines. *Bull Chem Soc Jpn*. 1938;13:252–60.
7. Bailes RH, Calvin M. The oxygen-carrying synthetic chelate compounds. VII. Preparation. *J Am Chem Soc*. 1947;69:1886–1893.
8. Suzuki M, Ishiguro T, Kozuka M, Nakamoto K. Resonance Raman spectra, excitation profiles, and infrared spectra of $[Co(salen)_2]O_2$ in the solid state. *Inorg Chem*. 1981;20:1993–1996.
9. Hester RE, Nour EM. Resonance Raman studies of transition metal peroxo complexes: 5-the oxygen carrier Cobalt(II)-salen and its μ-peroxo complexes, $[L(salen)Co]_2O_2$; L=DMSO, py, DMF, pyO, and no L. *J Raman Spectrosc*. 1981;11:49–58.
10. DeIasi R, Holt SL, Post B. The crystal structure of the oxygen-inactive form of bis(salicyladehyde)ethylenediiminecobalt(II). *Inorg Chem*. 1971;10:1498–1500.
11. Sharma AC, Borovik AS. Design, synthesis, and characterization of templated metal sites in porous organic hosts: application to reversible dioxygen binding. *J Am Chem Soc*. 2000;122:8946–8955.
12. Meier I, Pearlstein RM, Ramprasad D, Pez GP. Tetrabutylammonium tetracyanocobaltate(II) dioxygen carriers. *Inorg Chem*. 1997;36:1707–1714.
13. Hutson ND, Yang RT. Synthesis and characterization of the sorption properties of oxygen-binding cobalt complexes immobilized in nanoporous materials. *Ind Eng Chem Res*. 2000;39:2252–2259.
14. Wei M, Musie GT, Busch DH, Subramaniam B. CO_2-expanded solvents: unique and versatile media for performing homogeneous catalytic oxidations. *J Am Chem Soc*. 2002;124:2513–2517.
15. Musie GT, Wei M, Subramaniam B, Busch DH. Autoxidation of substituted phenols catalyzed by cobalt Schiff base complexes in supercritical carbon dioxide. *Inorg Chem*. 2001;40:3336–3341.
16. Sharma S, Kerler B, Subramaniam B, Borovik AS. Immobilized metal complexes in porous hosts: catalytic oxidation of substituted phenols in CO_2 media. *Green Chem*. 2006;8:972–977.
17. Welbes L, Borovik AS. Confinement of metal complexes within porous hosts: development of functional materials for gas binding and catalysis. *Acc Chem Res*. 2005;38:765–774.
18. Johnson CA, Sharma S, Subramaniam B, Borovik AS. Nanoparticulate metal complexes prepared with compressed carbon dioxide: correlation of particle morphology with precursor structure. *J Am Chem Soc*. 2005;127:9698–9699.
19. Dreisbach F, Lösch HW. Magnetic suspension balance for simultaneous measurement of a sample and the density of the measuring fluid. *J Therm Anal Calorim*. 2000;62:515–521.
20. Di Giovanni O, Dörfler W, Mazzotti M, Morbidelli M. Adsorption of supercritical carbon dioxide on silica. *Langmuir*. 2001;17:4316–4321.
21. Pini R, Ottiger S, Rajendran A, Storti G, Mazzotti M. Reliable measurement of near-critical adsorption by gravimetric method. *Adsorption*. 2006;12:393–403.
22. Martell AE, Calvin M. Bis-salicylaldehyde-imine oxygen carriers. In: *Chemistry of the Metal Chelate Compounds*. New York: Prentice Hall, 1952:339–352.
23. Aymes DJ, Paris MR, Mutin JC. Sur les complexes du Co(II) transporteurs d'oxygene a l'etat solide no 1 etude thermodynamique du systeme fluomine solide-oxygene gazeux. *J Mol Catal*. 1983;18:315–328.
24. Johnson CA, Long B, Nguyen JG, Day V, Borovik AS, Subramaniam B, Guzman J. Correlation between active center structure and enhanced dioxygen binding in Co(salen) nanoparticles: characterization by in situ infrared, Raman, and X-ray absorption spectroscopies. *J Phys Chem C*. 2008;112:12272–12281.
25. Borovik AS, Zart MK, Zinn PJ. Dioxygen binding and activation: reactive intermediates. In: Tolman WB, editor. *Activation of Small Molecules: Organometallic and Bioinorganic Perspectives*. Weinheim: Wiley-VCH, 2006:187–234.

Manuscript received May 21, 2008, revision received Aug. 22, 2008, and final revision received Oct. 8, 2008